

# Validation of a New Scoring System for the Detection of Early Forme of Keratoconus

Alain Saad, Damien Gatinel

## ABSTRACT

**Purpose:** To evaluate the accuracy of a new objective method for the detection of ectasia susceptible eyes.

**Methods:** One hundred and eighty-three elevation and placido topographies were retrospectively evaluated by one experimented refractive surgeon and classified as 'normal' or 'at risk for LASIK'. An objective automated system built on the combination of topography and tomography data in a discriminant function was also used to classify the corneas. The concordance between the objective and the subjective classification was evaluated and the usefulness of the objective scoring system was assessed by receiver operating characteristic (ROC) curve analysis.

**Results:** The mean age of the studied group was  $37 \pm 8$  years old. One hundred and fifty-nine eyes were subjectively classified as 'normal' and 24 as 'At risk for LASIK'. The scoring system correctly classified 153 eyes as 'normal' and 22 eyes as 'at risk for LASIK'. Six eyes were wrongly detected as 'at risk' by the automated system (false-positive) and two eyes were wrongly classified as 'normal' (false-negative). The sensitivity and specificity of the automated system were 92 and 96% respectively.

**Conclusion:** An automated system built on the combination of topography and tomography parameters can help in creating a sensitive and specific artificial intelligence for the detection of corneas at risk for refractive surgery.

**Keywords:** Keratoconus, Post-LASIK ectasia, LASIK complications, Keratoconus suspect, Artificial intelligence.

**How to cite this article:** Saad A, Gatinel D. Validation of a New Scoring System for the Detection of Early Forme of Keratoconus. *Int J Kerat Ect Cor Dis* 2012;1(2):100-108.

**Source of support:** Nil

**Conflict of interest:** None declared

## INTRODUCTION

Corneal ectasia is an uncommon but serious, vision-threatening complication of refractive surgery.<sup>1-9</sup> It is characterized by a progressive topographic steepening associated with irregular astigmatism and visual acuity loss. Its incidence varies in the literature between 0.01 and 0.9%<sup>3,10-13</sup> but is probably underestimated because its onset may be delayed 4 years after surgery.

By analyzing all the reported cases in the English literature as well as personal data, Randleman et al identified a variety of factors [topography, age, degree of myopia (M), residual stromal bed (RSB) and central pachymetry (CP)] and considered them in a weighted fashion to sort an ectasia

risk score.<sup>5</sup> Binder studied more than 9,000 eyes having at least one of the currently identified risk factors for ectasia (keratometry  $> 47$  D, RSB  $< 250$  microns, M  $> 8$  D, CP  $< 500$  microns and age  $< 25$  years) without any of them developing this complication postoperatively.<sup>10</sup> However, it was well-accepted by all the authors that abnormal preoperative topography and similarity to keratoconus suspect represent the most important independent risk factor for post-LASIK ectasia. There's a persistent ambiguity regarding the exact definition of a suspect keratoconus (KCS) cornea and there are no widely accepted criteria to categorize an eye as KCS.<sup>14-16</sup> We previously showed that studying the contralateral topographically normal eye of asymmetric keratoconus helps in creating a highly efficient artificial intelligence for the detection of the early form of keratoconus.<sup>17,18</sup> In the current study, we test the validity of this artificial intelligence system named score by applying it to a novel LASIK population.

## PATIENTS AND METHODS

We retrospectively evaluated 183 consecutive topographies of myopic patients that presented at the Rothschild Foundation for evaluation in 2008. These eyes were consecutive cases not included in the previous analysis to create the artificial intelligence system.<sup>18</sup> All these patients had a complete ophthalmic examination including manifest refraction, slit-lamp examination and fundoscopy. Placido and elevation topographies were performed using the OPD scan (Nidek, Japan) and the Orbscan (Technolas Perfect Vision, Germany) topographers. The topographies were classified by the authors as either 'suitable' or 'at risk' for LASIK surgery based only on the Placido and elevation maps. The magnitude of the myopic refractive error was not taken into account for this subjective classification.

The 'score' is an artificial intelligence system that uses a combination of Placido and tomography corneal indices obtained with the Orbscan system. The theory behind the score creation was already published.<sup>18</sup> The corneal indices are associated in a discriminant function to give a score to each cornea. A positive score ( $>0$ ) reflects a suspicious cornea or a cornea at risk for LASIK while a negative score ( $<0$ ) reflects a normal cornea. Each evaluated cornea was scored by the automated artificial intelligence system. The concordance between the subjective and the objective

classification was assessed by receiver operating characteristic (ROC) curves.

## RESULTS

Patient's demographics and corneal indices in each subgroup and in the population are listed in Table 1. Among the variables used for the score calculation, the thinnest pachymetry (TP), the difference between the central pachymetry and the thinnest pachymetry (CP-TP) and the thinnest point decentration (TPy) were statistically different between the subjectively classified 'at risk' group and the subjectively classified as 'normal' group. One hundred and fifty-nine topographies were subjectively judged as negative, out of which six had a positive score. The calculated specificity for the scoring classification system was 96%. Twenty-four topographies were subjectively judged as positive, out of which two had a negative score. The calculated sensitivity for the scoring classification system was 92% (Table 2). Eyes included in the group subjectively judged as positive had a mean score of  $0.45 \pm 0.90$  while eyes included in the group subjectively judged as negative had a mean score of  $-1.83 \pm 1.1$  and the difference between the two was significant.

## DISCUSSION

The results of this preliminary study validate the automated scoring system as an effective method for identifying topographies at risk for developing corneal ectasia after LASIK. The scoring system utilizes more than 10 Placido and tomographic indices in a weighted fashion to classify the corneas as suspect or normal. None of the eyes of the tested group of patients was included in the original group that was used for the score creation, which gives more power to the validation of this scoring system. This automated system reached a high sensitivity and specificity (92 and 96% respectively) for the detection of corneas at risk for refractive surgery.

**Table 2:** Subjective and objective (score) classification result and the calculated sensitivity and specificity of the automated scoring system

|                | Score positive | Score negative | Sensitivity/specificity |
|----------------|----------------|----------------|-------------------------|
| Judged suspect | 22             | 2              | 92%                     |
| Judged normal  | 6              | 153            | 96%                     |

Our results show that it corresponds well with trained clinician judgment. The score value can be used as a severity rating scale, based on corneal Placido and elevation topography indices. This scoring method is tied to the Orbscan topographers, but similar approach could be developed with other instruments that incorporate Placido, elevation and tomography data.

Beside the score value, the display associated with the score value associates several maps including the classic 'Quad map display' from the original Orbscan software, a radar map and two graphs related to pachymetry data (Fig. 2).

The radar chart plots the value of a selection of these indices used in the score algorithm. This plot consists of a sequence of equiangular radii radiating from a central point, with each radius representing one of the indices and having its own scale. A line is drawn connecting the data values with the final point connected back to the first to form a closed polygon. The polygon is filled using a color scale, where the limit for two standard deviations for the considered variable is yellow. This provides the clinician with a visually striking representation and help general perception of the values of the selected indices.

The variables used to build the radar maps are:

- The thinnest point value (microns) which corresponds to the minimal thickness of the corneal wall (using the manufacturer-suggested default acoustic factor of 0.92)
- The maximal posterior elevation (microns): This value corresponds to the maximal distance from the anterior elevation data to the computed best fit sphere in the 3 mm central zone.

**Table 1:** Patient's characteristics in the population and in each subgroup

|                      | Population       | Subjectively classified as 'at risk' | Subjectively classified as 'normal' |
|----------------------|------------------|--------------------------------------|-------------------------------------|
| N                    | 183              | 24                                   | 159                                 |
| Age                  | $37 \pm 8$       | $37 \pm 8$                           | $39 \pm 7$                          |
| Mean sphere          | $-3.8 \pm 2.3$   | $-3.1 \pm 2.2$                       | $-3.9 \pm 2.4$                      |
| Mean cylinder        | $-0.7 \pm 0.8$   | $-0.7 \pm 0.6$                       | $-0.7 \pm 0.8$                      |
| Irregularity at 3 mm | $1.1 \pm 0.1$    | $1.2 \pm 0.1$                        | $1.1 \pm 0.1$                       |
| TP                   | $539 \pm 38$     | $512 \pm 26^*$                       | $543 \pm 38^*$                      |
| CP-TP                | $3.6 \pm 3.2$    | $4.0 \pm 3.6^*$                      | $3.5 \pm 3.1^*$                     |
| TPy                  | $-0.27 \pm 0.24$ | $-0.32 \pm 0.24^*$                   | $-0.26 \pm 0.24^*$                  |
| MPE                  | $25 \pm 7$       | $24 \pm 7$                           | $25 \pm 7$                          |

TP: Thinnest pachymetry; CP-TP: Central pachymetry-thinnest pachymetry; TPy: Thinnest point decentration; MPE: Maximum posterior elevation; \*significant difference  $p < 0.01$



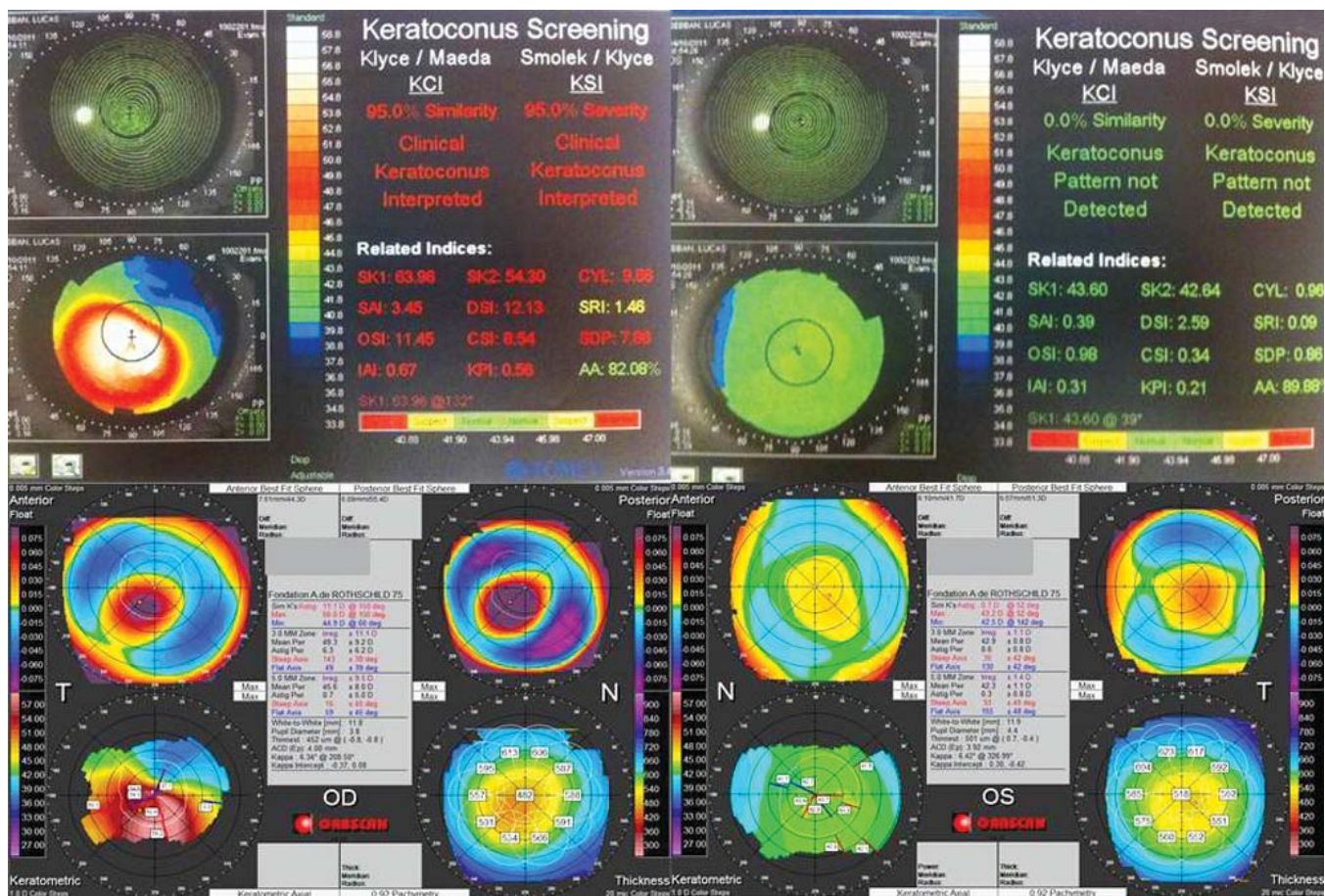


Fig. 1: Right and left placido (top) and elevation (bottom) topographies of a 21 years old man (TMS 4, Tomey, Japan). The top right and left images are the placido topographies revealing an evident keratoconus in the right eye but apparently normal cornea on the left eye

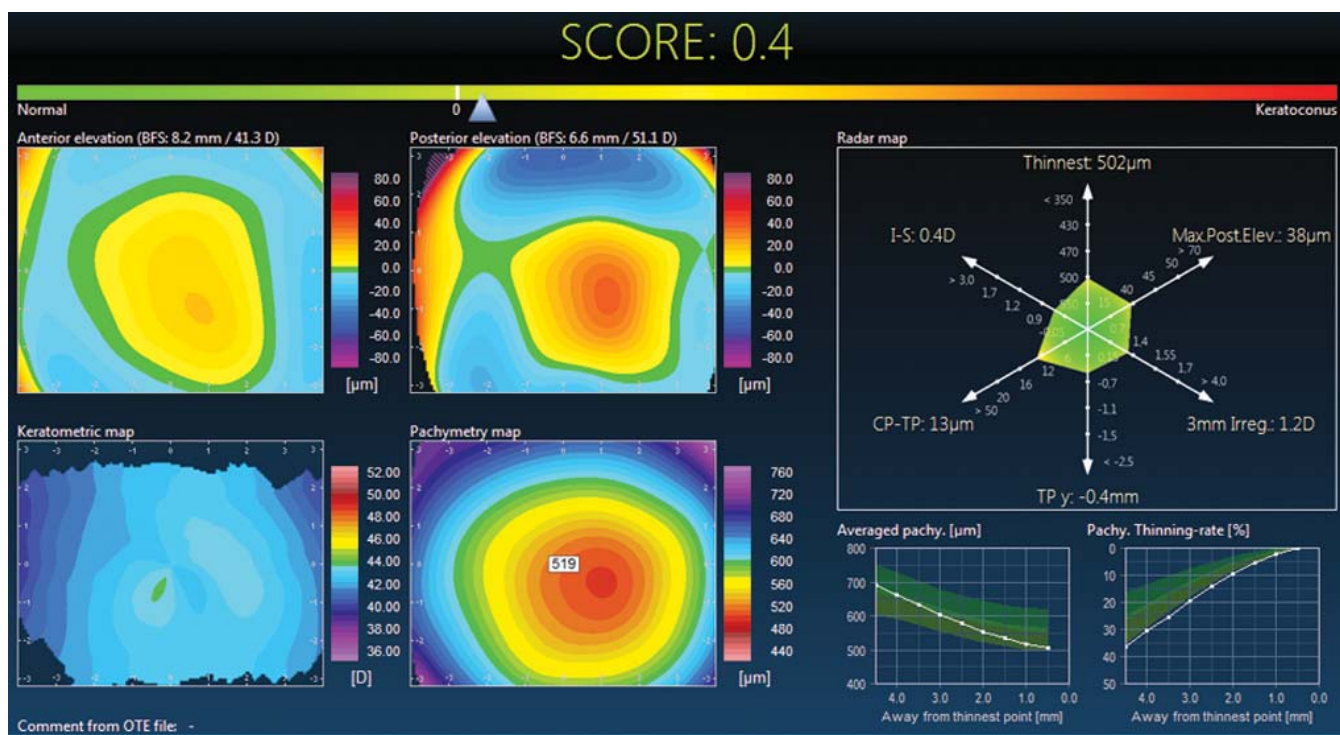


Fig. 2: Slightly positive score = 0.4 of the left cornea (same patient described in Figure1)

- The 3 mm irregularity (diopters): Optical surface irregularity is proportional to the standard deviation of surface curvature including the mean curvature, which is a measure of local surface sphericity and astigmatic curvature, both converted to dioptres by multiplying it by the surface keratometric index difference (0.3375).
- The vertical thinnest point decentration (mm) corresponds to the vertical displacement of the point of minimal pachymetry from the geometric center of the cornea.
- The difference between the central mean pachymetry and the thinnest pachymetry values (microns) is calculated by subtracting the value of the thinnest pachymetry to the value of the mean pachymetry within the 2 mm central zone.
- I-S value (D): It corresponds to the difference between the mean values of the Placido keratometry obtained from two groups of five equidistant points, located 1.5 mm from the vertex in the hemi-inferior (I) and hemisuperior (S) anterior corneal surface respectively. It quantifies the degree of vertical asymmetry of the anterior corneal surface.

Even if some of the corneal indices were statistically significantly different between the two groups [TP, CP-TP and the thinnest point decentration (TPy)] (Table 1), their clinical value is low if considered in isolation, as there is an important overlap between normal and abnormal values. In such case, it is preferable to associate the indices in a discriminant function to separate between the groups.

The display associated with the score value also includes a meridionally averaged thickness profile (averaged pachymetry) and percentage of thickness decrease (thinning rate) graphs, both plotted from the 9 mm peripheral ring to the thinnest point with regards to a normal band encompassing  $\pm 2$  standard deviations obtained from a control group. The x-axis represents the circle diameter centered on the thinnest point (0.0). The y-axis represents the corresponding thickness data in the averaged pachymetry graph and percentage of thinning from the periphery to the thinnest point in the 'thinning rate' graph.

## CONCLUSION

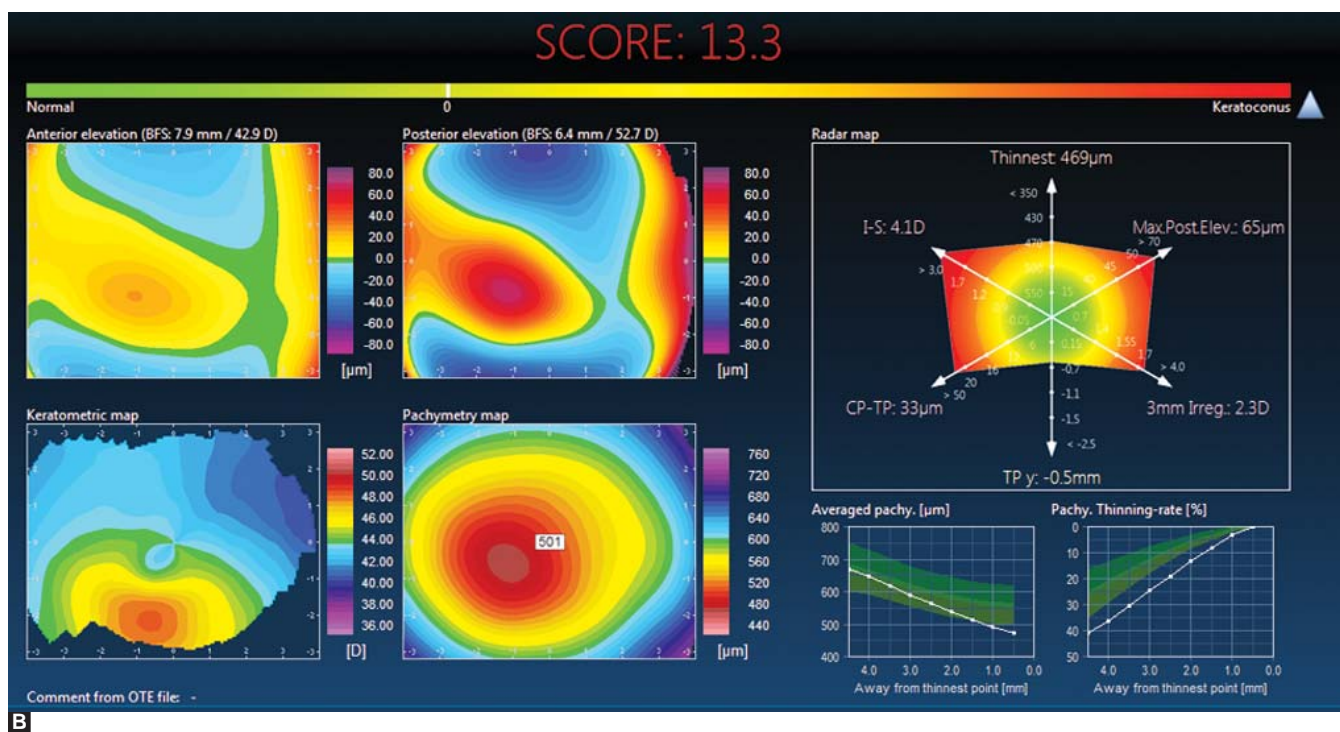
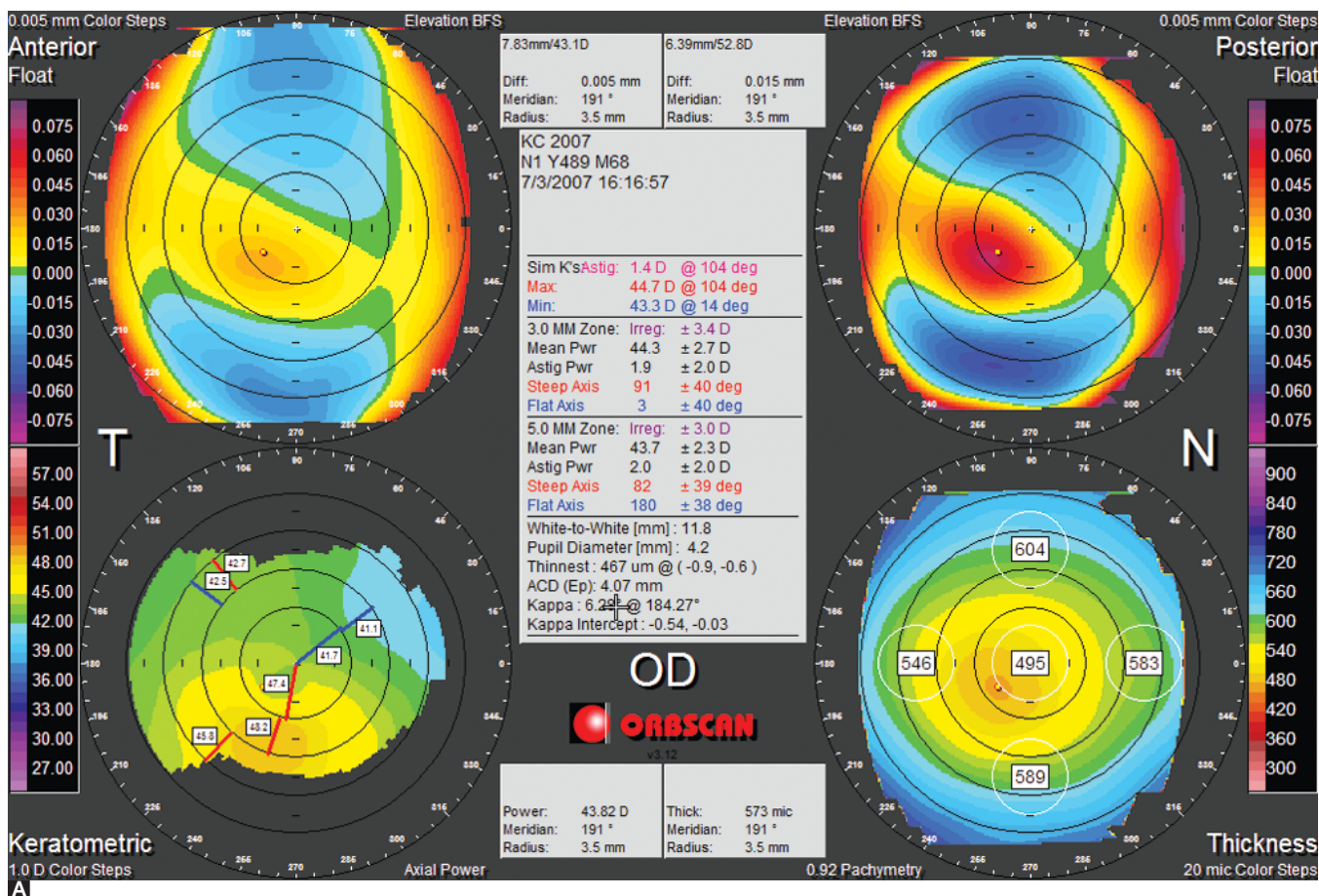
The new scoring system for the validation of keratoconus provides an objective measure which quantifies the status of the cornea with a single value (the score number). We found reasonable concordance between this objective and the subjective classification for early subclinical keratoconus detection.

The objective measure provided by the score can also be used to quantify the rate of progression of keratoconus, and assess the efficiency of keratoconus treatment by providing a geometry-based assessment of the effects of treatments, such as cross-linking.

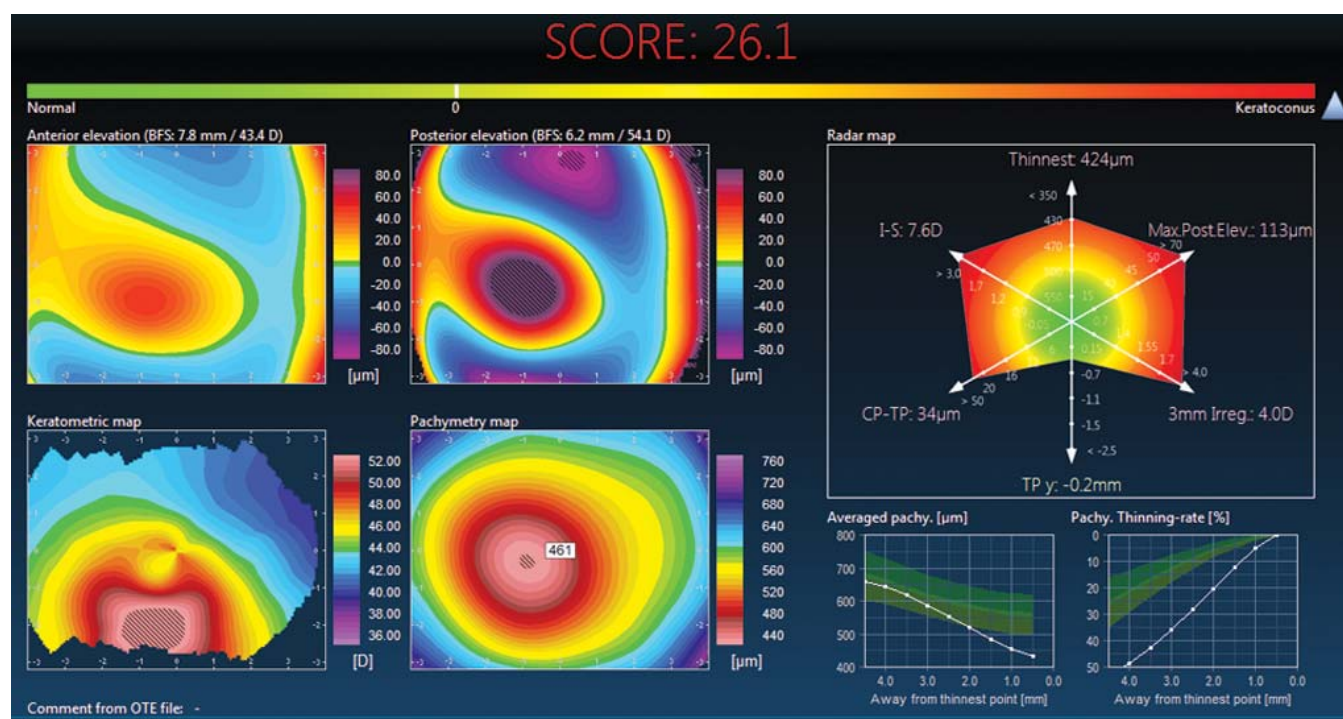
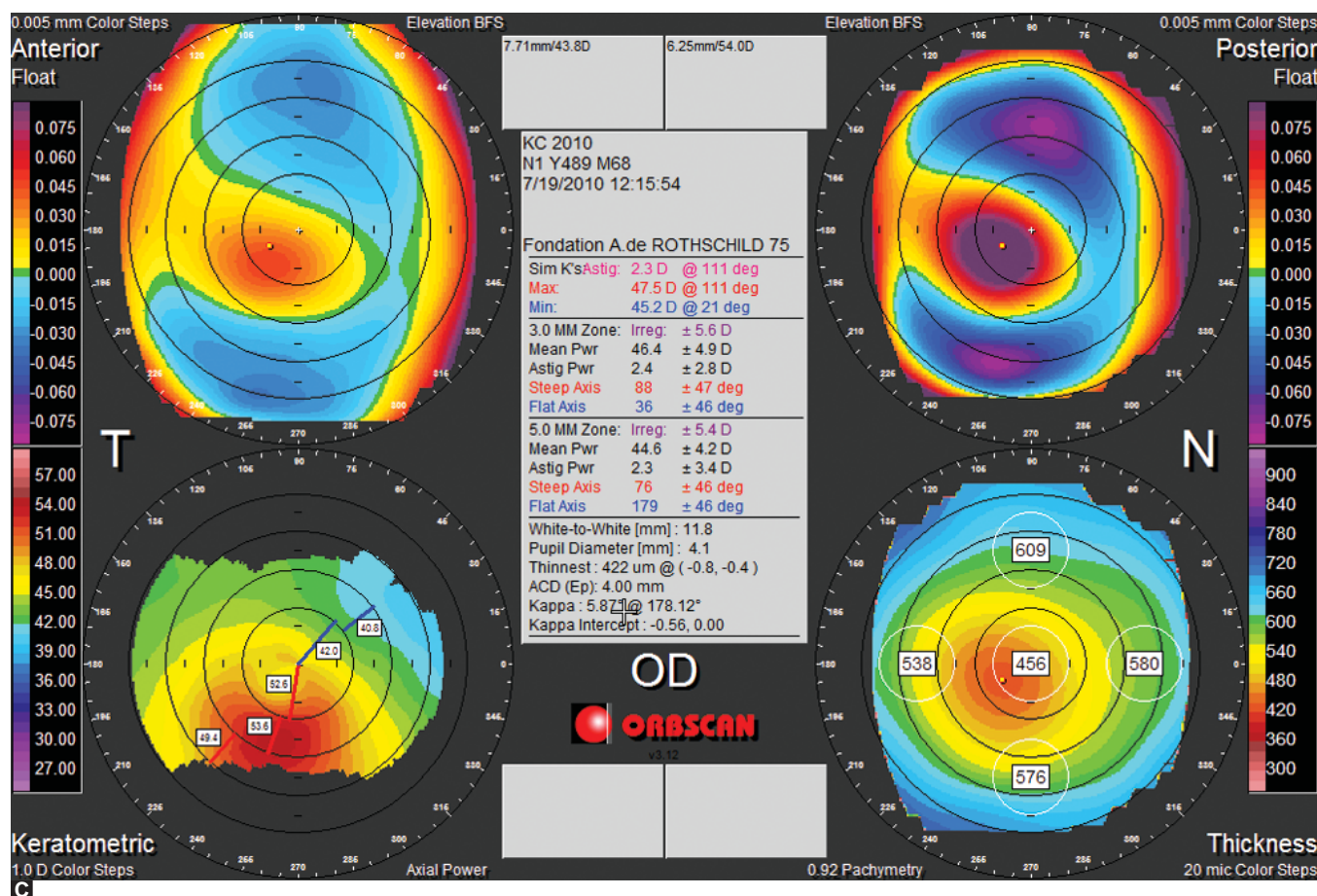
Figure 1 present the right and left Placido and elevation topographies of a 21 years old man. The top right and left images are the Placido topographies revealing an evident keratoconus in the right eye but apparently normal cornea on the left eye. The Klyce/Maeda and Smolek/Klyce automated system-based on Placido topography detects the keratoconus in the right eye. However, the percentage of similarity to keratoconus is 0% in the left eye. The left eye is a typical forme fruste keratoconus as it exhibits subtle topographic characteristics suggestive of an early subclinical keratoconus that are not pronounced enough to reach the threshold of keratoconus suspicion with Placido-automated classification. Keratoconus is a bilateral, progressive asymmetric disease; hence it is legitimate to postulate that the apparently normal cornea in an eye of patient who exhibits keratoconus in the contralateral eye may contain some indices that remain undetected by current automated Placido topography detection software. The score automated artificial intelligence system adds indices derived from tomography and elevation to Placido indices, in order to achieve better sensitivity and specificity for the detection of early form of subclinical keratoconus. Figure 2 presents the display associated with the slightly positive score (0.4) of this patient. Hence, the association of Placido and tomography indices allows the detection of this forme fruste keratoconus. In addition, the pachymetry thinning rate from the periphery to the center of the cornea was beside the 2 standard deviations of the mean values obtained from a normal population.

An objective scoring system is also useful for the evaluation of keratoconic corneas before any therapeutic approach. One can assess keratoconus progression using the objective scoring system which may be more reliable than the consideration of a single corneal indice. Figures 3A to D shows Orbscan quadmaps displays performed in 2007 and 2010 in an eye with keratoconus and the retrospectively calculated corresponding scores, revealing a clear progression of the keratoconus (score = 13.3 in 2007 and 26.1 in 2010). Similarly, Figures 4A to D suggests a stable keratoconus, as there are no variations of the score values calculated in 2009 and 2012 (score = 5.4 and 5.3 respectively).



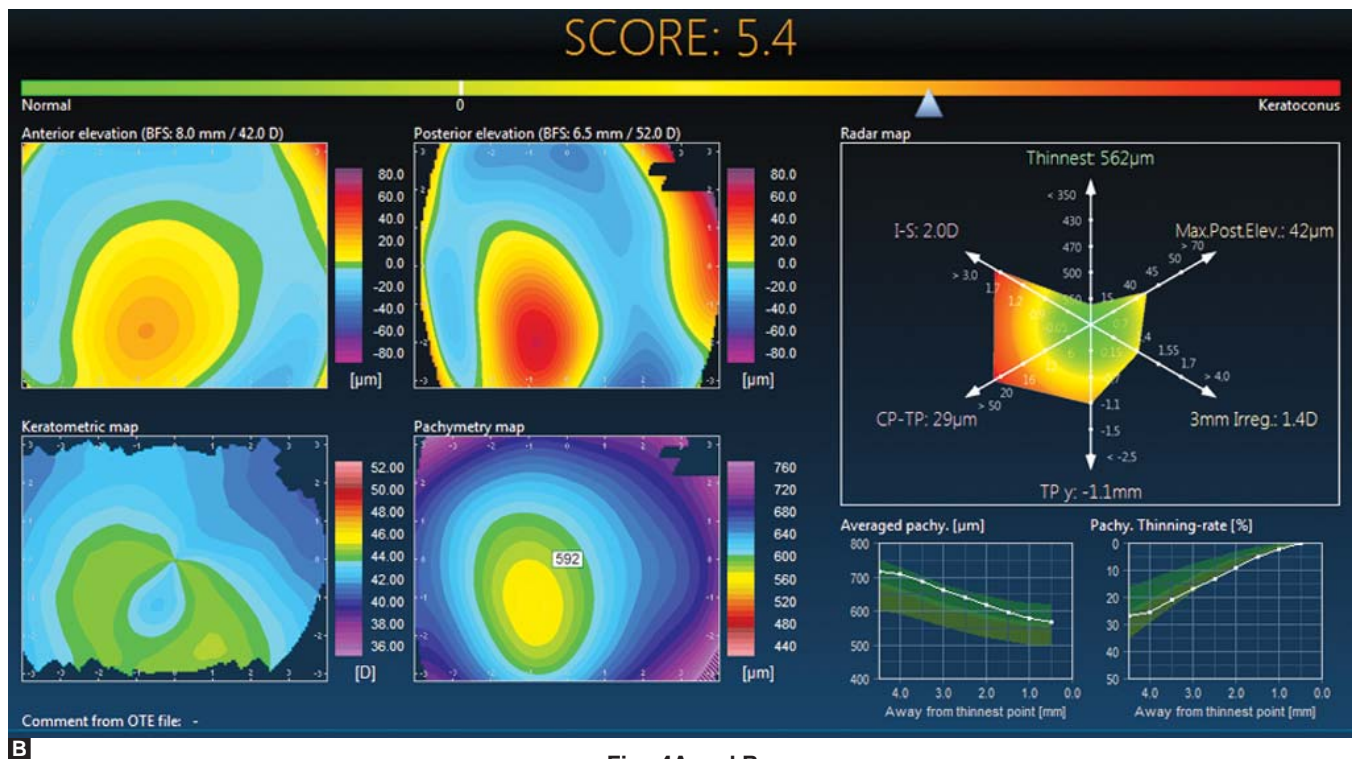
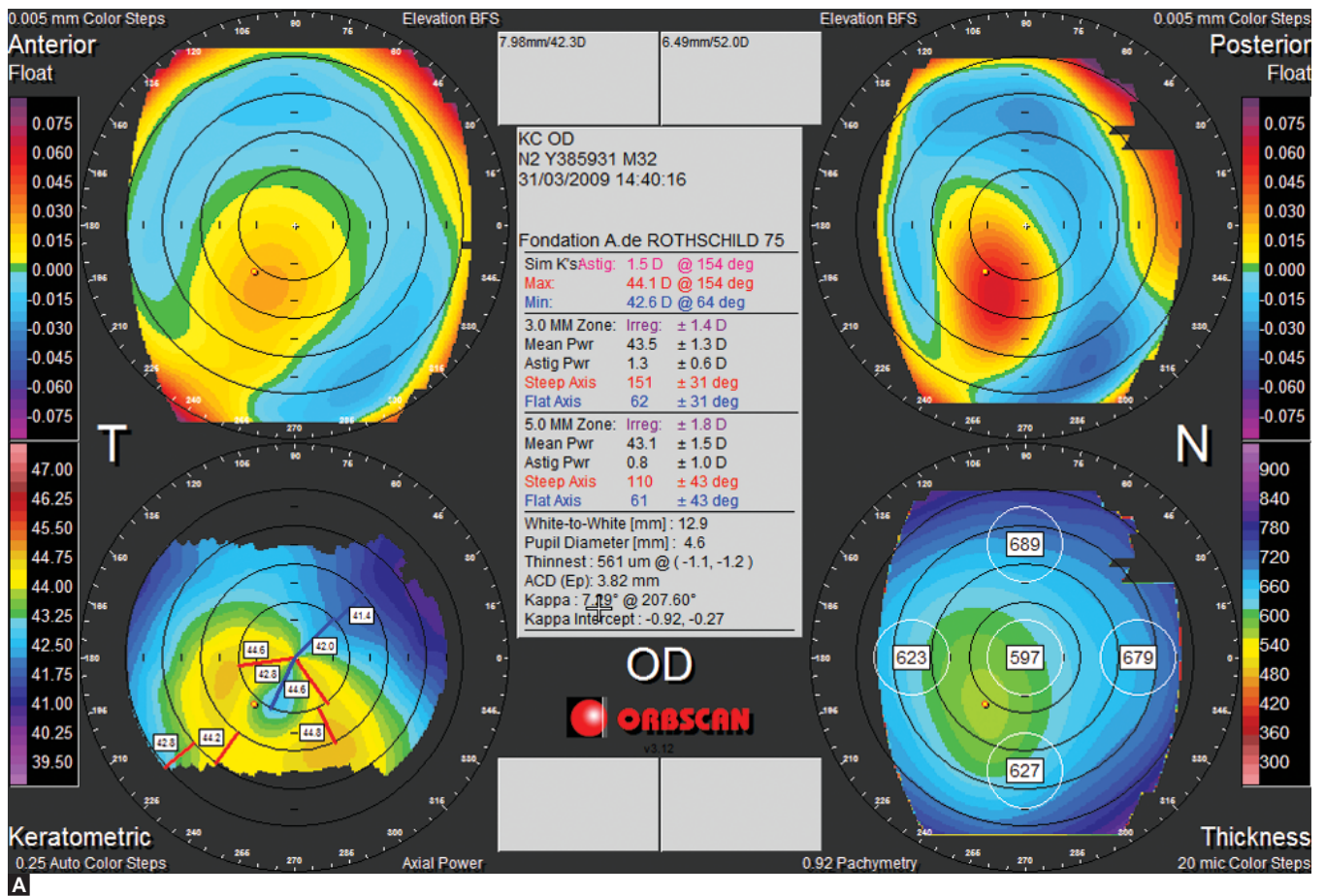


Figs 3A and B

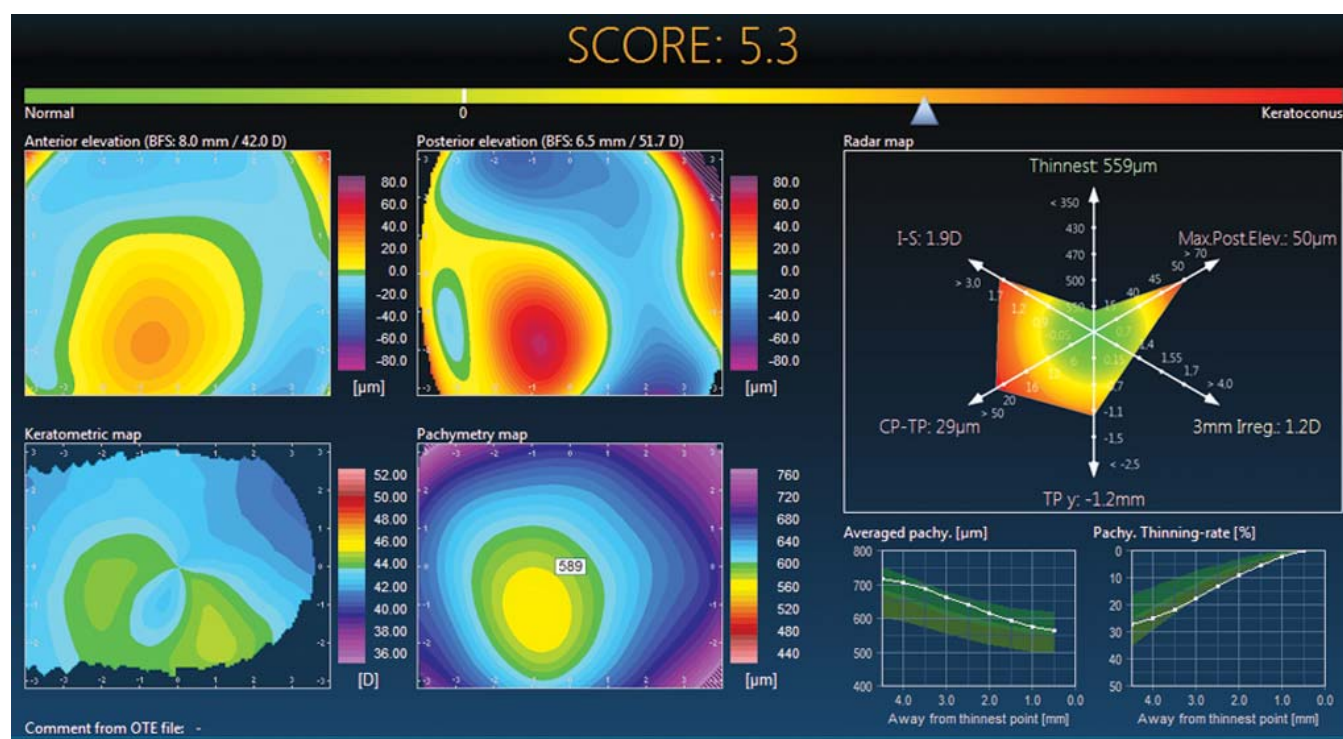
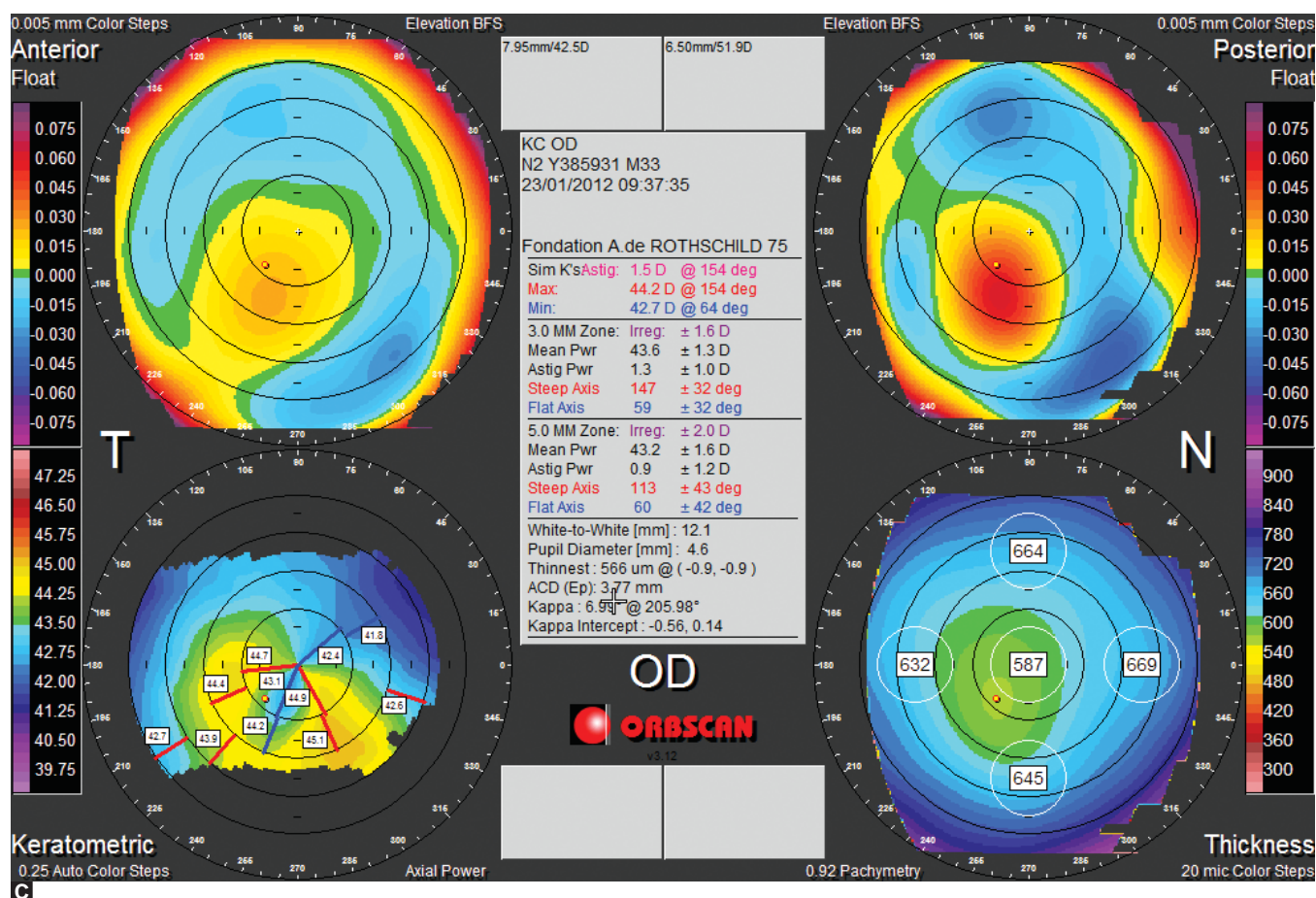


**Figs 3A to D:** Orbscan quadmaps performed in 2007 and 2010 on an eye with keratoconus and its corresponding score





Figs 4A and B



Figs 4A to D: Orbscan quadmaps in 2009 and 2012 in an eye with keratoconus and its corresponding score



## REFERENCES

1. Klein SR, et al. Corneal ectasia after laser in situ keratomileusis in patients without apparent preoperative risk factors. *Cornea* 2006;25(4):388-403.
2. Ou RJ, Shaw EL, Glasgow BJ. Keratectasia after laser in situ keratomileusis (LASIK): Evaluation of the calculated residual stromal bed thickness. *Am J Ophthalmol* 2002;134(5):771-73.
3. Pallikaris IG, Kymionis GD, Astyrakakis NI. Corneal ectasia induced by laser in situ keratomileusis. *J Cataract Refract Surg* 2001;27(11):1796-802.
4. Parmar D, Claoue C. Keratectasia following excimer laser photorefractive keratectomy. *Acta Ophthalmol Scand* 2004; 82(1):102-05.
5. Randleman JB, et al. Risk assessment for ectasia after corneal refractive surgery. *Ophthalmology* 2008;115(1):37-50.
6. Seiler T. Iatrogenic corneal ectasia after LASIK—is the end in sight?. *Klin Monbl Augenheilkd* 2005;222(5):429.
7. Saad A, Gatinel D. Association of corneal indices for the detection of ectasia-susceptible corneas. *J Refract Surg* 2012;28(3):166-67.
8. Saad A, et al. Retrospective testing of a new method for detecting ectasia-susceptible corneas. *J Cataract Refract Surg* 2011; 37(10):1907-08.
9. Saad A, Gatinel D. Bilateral corneal ectasia after laser in situ keratomileusis in patient with isolated difference in central corneal thickness between eyes. *J Cataract Refract Surg* 2010; 36(6):1033-35.
10. Binder PS. Analysis of ectasia after laser in situ keratomileusis: Risk factors. *J Cataract Refract Surg* 2007;33(9):1530-38.
11. Reinstein DZ, et al. Probability model of the inaccuracy of residual stromal thickness prediction to reduce the risk of ectasia after LASIK part II: Quantifying population risk. *J Refract Surg* 2006;22(9):861-70.
12. Rad AS, Jabbarvand M, Saifi N. Progressive keratectasia after laser in situ keratomileusis. *J Refract Surg* 2004;20(5 Suppl): S718-22.
13. Condon PI, O'Keefe M, Binder PS. Long-term results of laser in situ keratomileusis for high myopia: Risk for ectasia. *J Cataract Refract Surg* 2007;33(4):583-90.
14. Seiler T, Quurke AW. Iatrogenic keratectasia after LASIK in a case of Forme fruste keratoconus. *J Cataract Refract Surg* 1998; 24(7):1007-09.
15. Schlegel Z, Hoang-Xuan T, Gatinel D. Comparison of and correlation between anterior and posterior corneal elevation maps in normal eyes and keratoconus-suspect eyes. *J Cataract Refract Surg* 2008;34(5):789-95.
16. Klyce SD. Chasing the suspect: Keratoconus. *Br J Ophthalmol* 2009;93(7):845-47.
17. Saad A, Gatinel D. Evaluation of total and corneal wavefront high order aberrations for the detection of Forme fruste keratoconus. *Invest Ophthalmol Vis Sci* 2012;53(6):2978-92.
18. Saad A, Gatinel D. Topographic and tomographic properties of Forme fruste keratoconus corneas. *Invest Ophthalmol Vis Sci* 2010;51(11):5546-55.

## ABOUT THE AUTHORS

### Alain Saad

Ophthalmologist, Department of Ophthalmology and Anterior Segment Surgery, Rothschild Foundation, France

### Damien Gatinel (Corresponding Author)

Ophthalmologist, Department of Ophthalmology and Anterior Segment Surgery, Rothschild Foundation, France, e-mail: gatinel@gmail.com